

Introducing Distinctly Different Chemical Functionalities onto the Internal and External Surfaces of Mesoporous Materials**

Kristopher A. Kilian, Till Böcking, Katharina Gaus, and J. Justin Gooding*

There is currently considerable interest in mesoporous materials for a diverse range of applications, such as catalysis, filtration and separation, molecular collection and storage, nanofluidics, medical imaging, drug delivery, and sensors.^[1] To instill functionality into the raw materials, there is often a need for modifying the outside differently than the inside (e.g. targeted drug delivery: external antibodies for cell targeting, internal therapeutics for delivery). Recently, Cheng and Landry demonstrated spatial chemical selectivity on mesoporous silica by exploiting the slow diffusion in the nanoscale pores to ensure that the exterior is modified preferentially to the interior.^[2] This technique is a significant advance but does not ensure complete separation of the external modification layer from the internal modification layer. Thus, a need still exists for a general, material-independent methodology that will allow the interior of mesoporous materials to be modified with a specific chemistry while allowing a completely different, well-controlled chemical landscape on the external surface.

Herein we present a simple strategy towards achieving a sharp contrast in surface chemistry on the inside and outside of a mesoporous material. This approach relies on the combination of surface tension and capillarity to either prevent or promote the ingress of solution species inside the structure. As this method is dependent on surface tension, it relies on the hydrophobicity/hydrophilicity of the surface inside the pores relative to the solvent and on the pore size of the mesoporous structure and hence should be general for the modification of any mesoporous material. As a demonstration, we have used porous silicon (PSi) photonic crystals for two key reasons. Firstly, pore size is easily tuneable, and secondly, PSi can be engineered to exhibit a photonic band gap with high-quality optical properties.^[3] This latter feature is important, as it enables the chemical modification proceeding inside the structures to be monitored by shifts in reflectance spectra.^[4] To selectively derivatize the mesoporous

PSi, the physical characteristics of a hydrophobic functional monolayer at the entrance of mesopores are exploited on a previously reported PSi photonic crystal (a rugate filter^[4,5]). After forming a dense alkyl monolayer throughout the structure, the hydrophobicity of the mesopores was found to completely prevent the ingress of water. Capitalizing on this observation, the tops of the optical filters can be derivatized with aqueous solutions while leaving the bulk of the crystal unmodified. To functionalize the interior, the PSi is prewet with ethanol to allow infiltration of aqueous solutions; alternatively, organic solvents can be used. To demonstrate the utility of this chemical strategy we modified the exterior of a rugate filter with the peptide Gly-Arg-Gly-Asp-Ser (GRGDS), containing the cell-adhesive tripeptide Arg-Gly-Asp (RGD) for selective capture of cells, while modifying the interior with different chemical moieties (Figure 1). Cell adhesion was chosen as the test system, because some of the most promising applications for PSi photonic crystals are biophotonic sensing,^[4,6-9] “smart” implants,^[10-12] and targeted drug delivery,^[13] all of which require integration with live cells.

Rugate filters, prepared by anodization of Si(100) using a sinusoidal current profile, with pore sizes of approximately 12 nm,^[4] display a narrow linewidth and high reflectivity resonance in the reflectance spectrum (see Figure S2 in the Supporting Information). First, to stabilize the freshly etched silicon and introduce reactive functional groups, a monolayer was formed by thermal hydrosilylation of 10-succinimidylundecenoate, resulting in a 93-nm shift in the filter resonance as air in the porous scaffold was replaced with the Si-C linked monolayer (see Figure S2 in the Supporting Information). The PSi samples were immersed in water to evaluate the wetting behavior of the pores. The succinimide ester terminated monolayer produced a hydrophobic interface that completely prevents the infiltration of water,^[14] provided the surface was free of oxidized silicon (see Figure S1 in the Supporting Information).

Next, the top surface was derivatized by incubation in an aqueous solution of the peptide GRGDS (Figure 1 a, step 2 a) to provide a surface that promotes cell adhesion. The reflectivity spectra after this step displayed no change in the position of the optical resonance relative to before the modification, which indicates that there was no significant derivatization inside the pores (see Figure S2 in the Supporting Information). Likewise, transmission FTIR spectroscopy, a technique only sensitive to internal chemical modifications, indicated no change (see Figure S3 in the Supporting Information), again consistent with only the external surface being modified and the interior remaining unaltered.


Finally, as proof of principle for selective interior modification, the PSi structure containing RGD on the top was

[*] Dr. K. A. Kilian,^[†] Dr. T. Böcking,^[†] Prof. J. J. Gooding
School of Chemistry, University of New South Wales
Sydney 2052 (Australia)
Fax: (+61) 2-9385
E-mail: justin.gooding@unsw.edu.au

Dr. K. Gaus
Centre for Vascular Research, University of New South Wales
Sydney 2052 (Australia)

[†] These authors contributed equally to this work.

[**] The authors thank Michael Gal for helpful discussions. This work was supported by the Australian Research Council.

 Supporting information for this article is available on the WWW under <http://www.angewandte.org> or from the author.

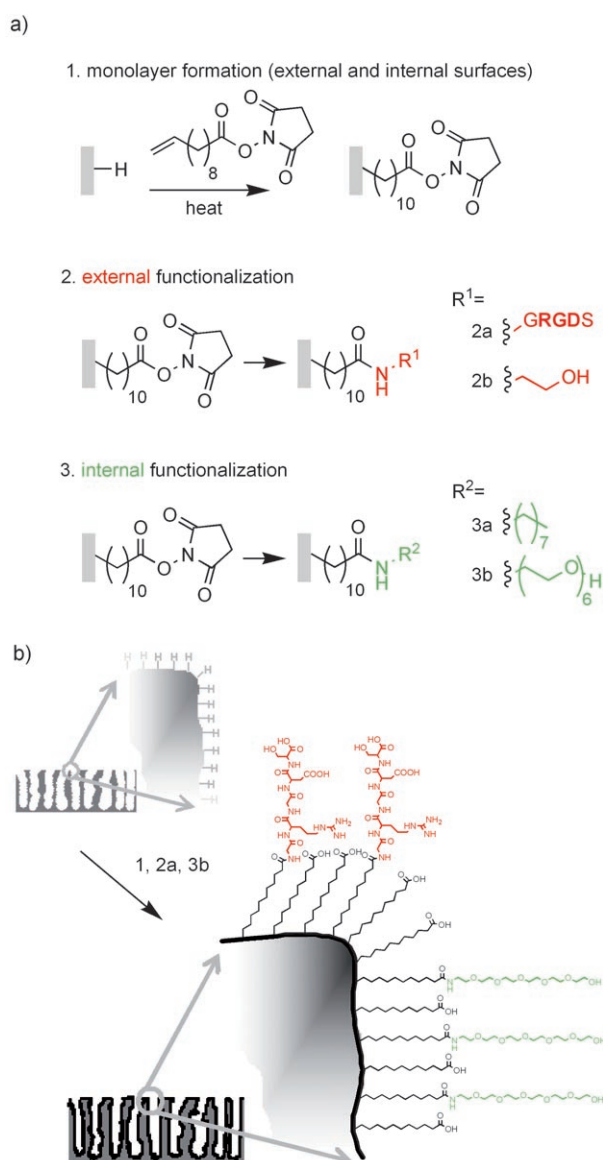


Figure 1. a) Procedure for modifying PSi with hydrophobic reactive monolayers by hydrosilylation of 10-succinimidylundecanoate and subsequent selective external and internal functionalization with different chemical moieties. b) Depiction of a pore tip before and after differential modification by steps 2a and 3b as an example.

cleaved in half. The interior of one half was reacted with octylamine (C_8) (Figure 1a, step 3a) and the interior of the other with hexa(ethylene glycol) amine (EG_6) (Figure 1a, step 3b), resulting in hydrophobic and hydrophilic interiors, respectively. Both reactions were performed in acetonitrile. In contrast to aqueous solutions, the organic solution infiltrates the structure by capillary action, and the amines can react with the *N*-hydroxysuccinimide (NHS) esters on the pore walls. This derivatization step was accompanied by a reflectivity shift of 10 nm for C_8 (Figure 2a) and 35 nm for EG_6 (Figure 2b), whereby the difference in the shifts reflects the difference in length and composition of the immobilized species. FTIR spectra also showed a loss of NHS ester peaks and appearance of clear amide bond signatures, as expected

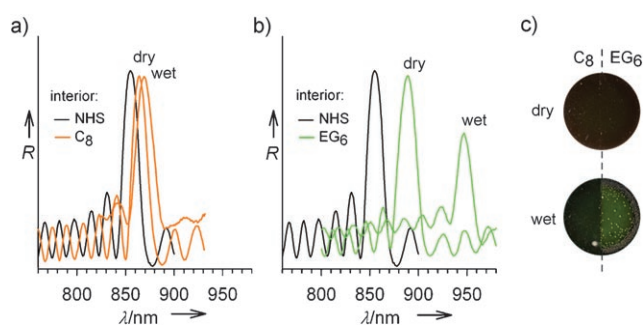


Figure 2. Shifts in the rugate filter resonance after derivatization: a) C_8 internal surface and b) EG_6 internal surface. c) Visual color change resulting from ingress of water (resonance at ca. 500 nm) into the structure with EG_6 internal surface.

for the coupling step inside the PSi (see Figure S3 in the Supporting Information).

The different internal surface coatings impart different physical properties on the photonic crystal. When water was applied to the surface, the PSi modified with the hydrophobic C_8 moieties displayed little evidence of the ingress of water, with a reflectivity shift of less than 5 nm (Figure 2a, “wet”). In contrast, the surface containing a hydrophilic EG_6 -terminated interior yielded a 56-nm shift (Figure 2b, “wet”), consistent with the pore space being completely filled with water. The spectral properties of the PSi in Figure 2a, b were engineered in the near-IR region (the so-called tissue window) with a view for these materials to be applicable for *in vivo* biophotonic applications. To demonstrate the fabrication flexibility and to allow easy evaluation of differential internal functionality, we also fabricated photonic crystals with optical properties in the visible region (same pore size and chemistry), such that infiltration of water could be observed visually by a color change (Figure 2c).

We used cell adhesion to test our approach for selectively modifying the top surface of the rugate filter. The top surfaces of two PSi rugate filters were functionalized with the peptide GRGDS (Figure 1, step 2a) and ethanolamine (Figure 1, step 2b), respectively. Both samples were treated with the same hydrophobic species (octylamine) on the interior to prevent ingress of water. The PSi samples terminated with the different external surface species were incubated with endothelial cells in serum-containing media. The cells were able to spread only on the surface displaying the RGD ligand and formed focal adhesions revealed by immunolabeling of paxilin (Figure 3a). The PSi containing a distal RGD moiety showed more than ten times the number of adherent cells compared to the surface passivated with ethanolamine (Figure 3b). Furthermore, cells imaged on the ethanolamine-terminated surface are predominantly round in shape, suggesting that there was no formation of focal adhesions. Thus, the successful specific modification of the exterior surface with different chemical moieties can be clearly distinguished by the adhesive behavior of cells.

After cell attachment, the samples were dried and the photonic signature was measured. The RGD-terminated samples, with many adherent cells, displayed a marked red shift in the reflectivity maximum of 35 nm relative to the

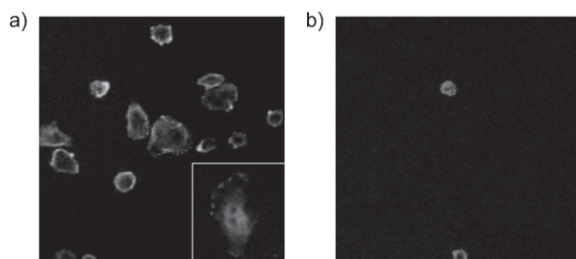


Figure 3. Endothelial cell adhesion on a) rugate filter with RGD-functionalized exterior and b) hydroxyl-terminated exterior. The inset in (a) shows a single cell with well-defined focal adhesions.

ethanolamine-coated samples with few cells. The shift to longer wavelengths in the presence of endothelial cells is attributed to the ingress of cellular material into the porous matrix and its deposition onto the pore walls. This observation demonstrates the potential of photonic crystals modified with different chemical moieties on the internal and external surfaces towards optically detecting cellular processes.

In summary, we have presented a differential functionalization procedure that capitalizes on the water-repellent behavior of hydrophobic monolayers in mesoporous materials. It could be possible to tailor the tendency for water exclusion by adjusting the pore size or the hydrophobicity of the monolayer to selectively modify the mesoporous materials. In Figures S4 and S5 in the Supporting Information, we demonstrate this principle with PSi with pore sizes in the range of 30–70 nm. Selective cell capture was demonstrated as a step towards biophotonic devices, but the inherent flexibility of this approach will allow for diverse functional moieties on the exterior, leaving the interior available for immobilizing any amine or alcohol of interest. This general method is amenable to microparticle fabrication^[15] for specific cell targeting and “smart” drug delivery and should prove applicable to other surface chemistries and porous materials. In conclusion, control over the interior and exterior surface chemistry will have a broad impact for the study and application of mesoporous materials.

Experimental Section

Experimental details of the materials, rugate filter preparation, monolayer formation, endothelial cell capture, and spectroscopy can be found in the supporting information.

Received: October 16, 2007

Published online: February 22, 2008

Keywords: cell adhesion · mesoporous materials · monolayers · surface chemistry

- [1] *Nanotechnology in Mesoporous Materials*, Vol. 146 (Eds.: S.-E. Park, R. Ryoo, W.-S. Ahn, C. W. Lee, R. Chang), Elsevier, Amsterdam **2003**, pp. 1–815.
- [2] K. Cheng, C. C. Landry, *J. Am. Chem. Soc.* **2007**, *129*, 9674–9685.
- [3] W. Theiss, *Surf. Sci. Rep.* **1997**, *29*, 91–192.
- [4] K. A. Kilian, T. Böcking, S. Ilyas, K. Gaus, M. Gal, J. J. Gooding, *Adv. Funct. Mater.* **2007**, *17*, 2884–2890.
- [5] S. Ilyas, T. Böcking, K. Kilian, P. J. Reece, J. Gooding, K. Gaus, M. Gal, *Opt. Mater.* **2007**, *29*, 619–622.
- [6] S. C. Bayliss, L. D. Buckberry, I. Fletcher, M. J. Tobin, *Sens. Actuators A* **1999**, *74*, 139–142.
- [7] S. Ben-Tabou de Leon, A. Sa’ar, R. Oren, M. E. Spira, S. Yitzchaik, *Appl. Phys. Lett.* **2004**, *84*, 4361–4363.
- [8] M. P. Schwartz, A. M. Derfus, S. D. Alvarez, S. N. Bhatia, M. J. Sailor, *Langmuir* **2006**, *22*, 7084–7090.
- [9] K. A. Kilian, T. Böcking, K. Gaus, J. J. Gooding, *ACS Nano* **2007**, *1*, 355–361.
- [10] L. T. Canham, C. L. Reeves, J. P. Newey, M. R. Houlton, T. I. Cox, J. M. Buriak, M. P. Stewart, *Adv. Mater.* **1999**, *11*, 1505–1507.
- [11] K. A. Kilian, T. Böcking, K. Gaus, M. Gal, J. J. Gooding, *Biomaterials* **2007**, *28*, 3055–3062.
- [12] Y. Y. Li, F. Cunin, J. R. Link, T. Gao, R. E. Betts, S. H. Reiver, V. Chin, S. N. Bhatia, M. J. Sailor, *Science* **2003**, *299*, 2045–2047.
- [13] F. Cunin, Y. Y. Li, M. J. Sailor, *BioMEMS Biomed. Nanotechnol.* **2006**, *3*, 213–222.
- [14] J. T. C. Wojtyk, K. A. Morin, R. Boukherroub, D. D. M. Wayner, *Langmuir* **2002**, *18*, 6081–6087.
- [15] M. J. Sailor, J. R. Link, *Chem. Commun.* **2005**, 1375–1383.